Cite this paper: ***M. Stroobach, L. Haya and M. Fenech, Medical Engineering and Physics 69 (2019) 100–108 https://doi.org/10.1016/j.medengphy.2019.04.008***

Effects of red blood cell aggregation on microparticle wall adhesion in circular microchannels

Mark Stroobach

Department of Mechanical Engineering, University of Ottawa, Ottawa, Canada.

mstro012@uottawa.ca

Laura Haya

Department of Mechanical Engineering, University of Ottawa, Ottawa, Canada.

Laura.haya@uottawa.ca

Marianne Fenech

Department of Mechanical Engineering, University of Ottawa, Ottawa, Canada.

mfenech@uottawa.ca

ABSTRACT

The wall adhesion of 1 μm microparticles in human blood was studied in circular microchannels. The level of particle wall adhesion was measured for varying levels of shear rate and varying degrees of red blood cell aggregation, which was modulated by the addition of macromolecule dextran 500. The blood preparations were injected into PDMS microfluidic devices that were modified to have circular channels, better matching the geometry of physiological microcirculation compared to square channels or Couette flow systems. The circular walls of the microchannels were embedded with biotinylated phospholipids to which marginating microspheres coated with streptavidin bound. The particle wall adhesion was evaluated by counting the particles that adhered to the channel's wall after flushing the channel. Blood preparations of five dextran concentrations (including baseline case of 0%) were tested for four flow velocities, to quantify the effects of aggregation for varying shear rate. It was found that the level of particle wall adhesion was positively correlated with the level of RBC aggregation, particularly at low shear rates, when aggregation was enhanced. The particle adhesion was especially enhanced at aggregation levels in the range of physiological aggregation levels of whole blood, suggesting that RBC aggregation plays an important role in the dynamics of platelets and leukocytes *in vivo*.

1 INTRODUCTION

Margination, the radial migration of particles in a channel flow towards the channel walls, which could result in the attachment of the particles to the wall, is an important feature of the microcirculation. The margination of platelets and leucocytes towards the vessel endothelium, and by extension their adhesion, is essential to their functions in wound healing, maintaining homeostasis, and the body's immune response to inflammation and infection [1]. Margination and wall adhesion are also important to drug delivery, since drug-carrying particles must come into close proximity with the vessel walls in order to be absorbed by the tissue. An advanced understanding of the mechanisms involved in particle margination and adhesion *in*

vivo could lead to improved drug design for targeted delivery [2]. Margination also has important applications *in vitro*; some lab-on-a-chip devices, for example, use the phenomenon to separate cells such as different blood components, or healthy cells from diseased ones [3,4].

Particle margination could be assessed by reporting the distribution of the particles across the channel radius, i.e. the local particle concentration [ref]. Usually, in blood the concentration is measured close the wall as the core of the vessel is occupied by RBCs. Such measurements require the use of fluorescent confocal microscopy. An alternative is to measure the particles that have attached to the wall, which is correlated to the particle margination[ref].

Margination is a complicated physical phenomenon influenced by the size, shape, density and stiffness of the marginating particles, as well as by the fluid shear rate, vessel geometry, and the concentration and aggregation tendency of the surrounding red blood cells [1]. While leukocytes, platelets and nanoparticles have all been shown to marginate in blood flow, their marginating behaviours are not affected equally by the blood flow variables. Margination is the result of a balance of forces acting on the particles - namely gravity, buoyancy, fluid drag, van der Waals and Brownian forces - causing their net lateral movement away from fluid streamlines [1]. As particle size increases, this force balance changes, with gravity and fluid drag becoming increasingly important, whereas for very small particles (<500 nm) Brownian motion and colloidal forces dominate. Charoenphol *et al.* found that for spheres 0.5 to 10 μm in diameter, margination increased with increasing particle size [5]. In general, non-spherical particles have a higher tendency to marginate than spherical ones [1].

Nobis *et al.* found that leukocyte margination was negatively correlated with shear rate [6]. Conversely, Tilles and Eckstein, and Aarts *et al.* found that the margination of smaller platelets or beads in RBC suspensions flowing in glass capillaries increased with shear rate [7,8]. Yeh. and Eckstein , on the other hand, found that in high hematocrit suspensions (H=40%), the margination of platelet-sized spheres was maximum at some optimal shear rate, suggesting that the shear-marginating relationship is more complex [9].

From early experiments of blood in glass capillaries, Vejlens was the first to correlate the margination of leukocytes with RBC aggregation [10]. While it has been found that RBC aggregation is not necessary for WBC margination to occur [11,12], from their 2D numerical simulation of Fedosov showed that it does strengthen it [11]. Likewise, Pearson and Lipowsky found RBC aggregation to be positively correlated with leukocyte margination in venules in rat mesentery [13]. They found this effect was most prominent at higher hematocrits and shear rates, and attributed it to tighter RBC packing when aggregated (i.e. a less dispersed RBC core) which inhibited the white blood cells from lifting off away from the wall. This finding may explain a mechanism of the body's immune response: inflammatory conditions *in vivo* have been found to promote abnormal hyper RBC aggregation – this correlation suggests that this may be in order to force more leukocytes toward the endothelium where they are needed to respond to the inflammation.

The effect of RBC aggregation on platelet margination is less conclusive. Woldhuis *et al.* found that by increasing RBC aggregation in rabbits (by addition of dextran 500), platelets became more centrally distributed in arterioles; i.e., opposite to the findings for leukocytes, platelet margination was negatively correlated with RBC aggregation [14]. They found no correlation, however, in venules. Guilbert *et al.* , however, conversely found that in Couette flow, 2 μm spheres (comparable in size to platelets) adhered more to the Couette wall with increasing RBC aggregation [15]. This result was consistent for three hematocrits (20%, 40%, 60%), and two shear rates tested (2 s^{-1} and 10 s^{-1}). These contrasting results raise questions about the effects of other factors including the shape and flexibility of platelets compared to sphere surrogates, the endothelial receptors and strength of bond, and the effects of the channel geometry and associated shear profiles. It is necessary to investigate these variables independently in order to delineate their effects.

Jain and Munn showed that channel size indeed affects the marginating behaviour of WBCs, with margination decreasing with increasing channel width in rectangular channels [16] (this is consistent with findings of Goldsmith and Spain in glass capillaries [17]), and increasing at sudden expansions. Yang *et al.* reported the effect of channel cross-sectional geometry on leukocyte margination and found that

leukocyte trajectories were drastically influenced by the channel cross-section when flowing in bifurcating microchannels with either rectangular or rounded cross-sections [18]. In the rectangular channels, the WBCs marginated preferentially towards the corners, which effected their distribution between the bifurcating branches. This finding emphasized the importance of modelling anatomically accurate channel geometries when modeling microcirculatory flows.

These effects of varying geometry on the margination of different particle sizes are coupled with the differences in shear rate profiles associated with the geometry, which as discussed above, have a strong influence on particle margination. For example, leukocytes have been found to marginate more in post-capillary venules than in arterioles, whereas platelets were found to marginate more in arterioles [2]. This may be a consequence of the sensitivity of the different particle characteristics (size, shape and flexibility) to the different shear rates and geometries present in arterioles *vs.* venules. RBC aggregation is another coupled variable, as it increases at low shear rates and is inhibited at shear rates greater than 100-120 s^{-1} [19].

In summary, with many variables at play, the detailed mechanisms of micro-particle margination remain unclear. No study has been done to our knowledge investigating the effects of RBC aggregation on platelet-sized particles in circular microchannels. Assuming wall adhesion being proportional to the margination, the objectives of this research are to quantify the effects of RBC aggregation on micro-particle wall adhesion (1µm spheres) under physiological arteriole flow conditions within round microchannels, under varying physiological levels of shear rate. methods

1.1 Channel fabrication

Circular microchannels were fabricated in PDMS. Using a method introduced by Yang *et al.* [18], this was done by first fabricating channels having approximately square cross-sections, which were used as scaffolds filled in a second step to have circular cross-sections (Figure 1). The liquid PDMS used in the second step was mixed with biotinylated phospholipids, embedding the channel walls with functionalized

biotin groups to which the marginating microspheres, coated in streptavidin, would strongly bind. The square scaffold channels were fabricated using a standard procedure, outlined briefly in the following. The resulting channel geometries on the master mold had dimensions 1.00 cm long, 106 μm in height and 116 μm in width.

PDMS pre-polymer and a curing agent were mixed together at a ratio of 10:1. The mixture was degassed (72 kPa for one hour) and poured onto the channel master and baked on a hot plate (30 min at 135°C). Once removed from the mold, the PDMS was cut into individual chips and holes were punched through at the inlets and outlets. The cast PDMS sections were then bonded to another flat piece of PDMS using an Oxygen Plasma etcher (PE-50: Plasma Etch Inc., Carson City, USA) to enclose the channels.

The square PDMS microchannels were then filled with biotinylated liquid PDMS to create rounded channels. One milliliter of liquid PDMS was combined with 7.5 μL of a 5 mg/mL phospholipid–chloroform solution. The biotinylated liquid PDMS was injected into the square channels with a syringe. A stream of compressed air (5 psi/cm) was injected through the microchannels, while curing on a hot plate at 100°C for 20 minutes, forcing the liquid PDMS out and leaving a circular channel. In order to fully cure the deposited PDMS coating, the channel was baked for an additional 20 minutes at 100°C with no compressed airflow.

The channel diameters were measured by cutting off the end portion of each channel, and imaging its cross section under the microscope. The average diameter D was taken as the average of two orthogonal measurements, D_1 and D_2. Over 50% of the channels that were made using this procedure had near-circular cross-sections (Figure 2 (b)), as judged by the ratios of D_1/D_2. This result was considered satisfactory, given that individual channels were examined prior to being used for the experiments to ensure that they were circular. The average channel diameter was 85 ± 7μm.

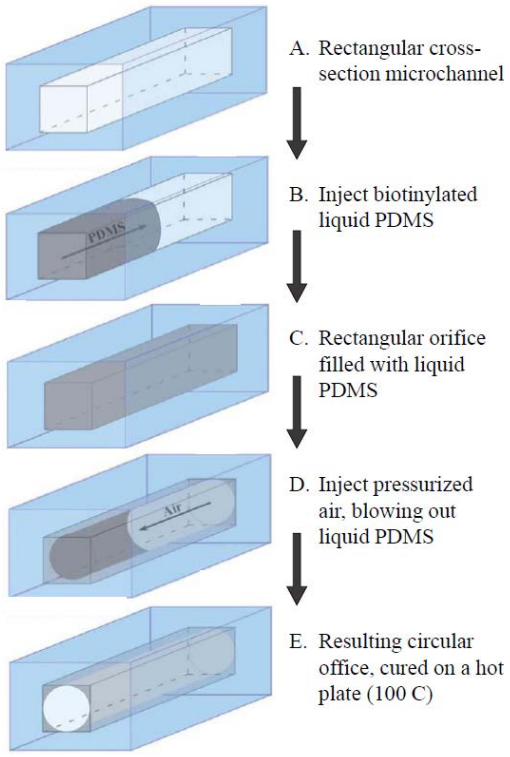

Figure 1. Steps in creating a round channel in PDMS. Modified from Yang *et al.* [18].

1.2 Measurement of particle adhesion

Human blood was collected from volunteers by Gamma Dynacare laboratories (Ethics reference number: H11-13-06). A standard procedure for blood separation was used: the blood samples were centrifuged at 3000 rpm for 10 minutes, the plasma and the buffy coat were extracted and discarded, and phosphate buffered saline (PBS) was added to the remaining red blood cells to wash them. This was repeated twice more. The cleaned RBCs were suspended in a solution of PBS with 27%v/v of Optiprep™ Density Gradient Medium (MFCD00867965: Sigma-Aldrich, St. Louis, USA) to achieve hematocrits of 10%. The Optiprep™ was added to increase the density of the suspending medium to minimize sedimentation during the experiment. Five different solutions were prepared from each suspension mixture, having 0%, 0.5%, 1.0%, 1.5% and 2.0% w/v concentrations of dextran 500 (AAJ63702-22: VWR International, Radnor, USA).

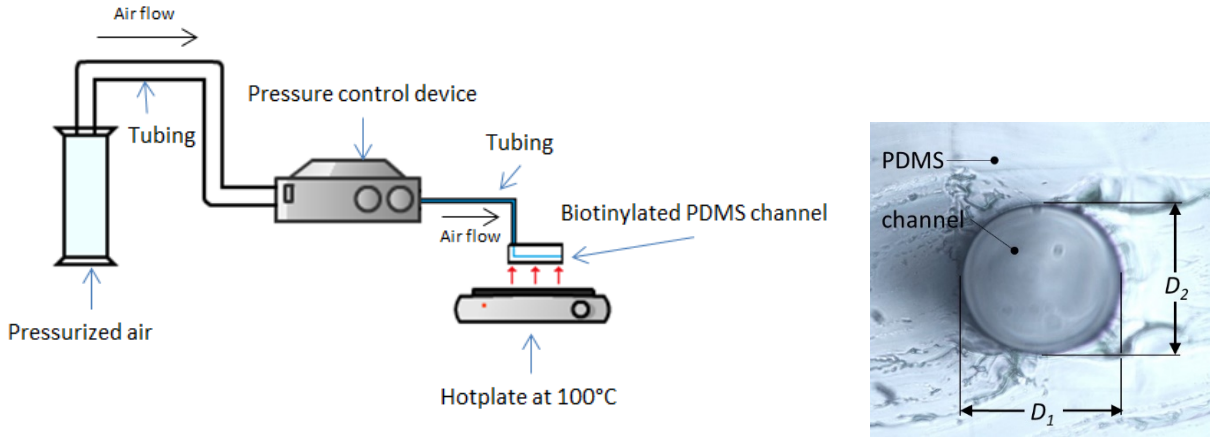

(a) (b)

Figure 2. (a) Diagram of air pressure set-up used to create circular channels: Pressurized air first leaves its storage and flows into the pressure control device, which ejects air at a controlled pressure of 5psi per cm of channel length. The controlled air flows into the channel while it is heated at 100°C and pushes the injected liquid biotinylated PDMS out to make a circular channel. (b) Cross-section of a typical round microchannel, imaged under a microscope. Characteristic diameter D was taken as the average of the two orthogonal diameter measurements, D_1 and D_2.

Fluorescent particles, 1 µm average diameter, coated with streptavidin (Excitation: 480nm, Emission: 520nm, CP01F-12884: Bangs Laboratories, Fishers, USA) were added to the blood suspensions at a concentration of 27 µL of particle solution per mL of sample fluid. The blood preparations were sonicated for three minutes (ultrasonic bath RK-08848-10: Cole-Parmer, Montreal, Canada) to break up any clumps of particles, to ensure that the particles would be dispersed homogeneously throughout the solution. These particles were chosen for their comparable size to platelets.

RBC aggregation levels were measured for each suspension of varying dextran concentration under static conditions using an aggregometer (RheoScan-AnD 300 System: RheoMeditech Inc., Seoul, Korea). Because the aggregometer uses light intensity passing through the sample to measure the aggregation level, the hematocrit of the samples must be near physiological levels to obtain an accurate reading: for samples

having too low hematocrit, too much light would pass through the sample, resulting in overexposure and inaccurate readings. For this reason, we used suspensions of 45% hematocrit to establish the relationship between dextran concentration and aggregation, instead of the 10% hematocrit used in the flow experiment. We also note that false positive measurements were obtained for samples of 0% dextran, as the measurement mechanism requires some level of aggregation to operate; however, unlike the aggregating samples, for which the measured light intensity passing through the sample increased in time as the RBCs aggregated, the measured light intensity for the 0% samples continually decreased. For this reason, the aggregation indices of the 0% dextran samples were set to zero.

A syringe pump (Nexus 3000: Chemyx Inc., Stafford, USA) controlled the flow rate of the blood samples through the microchannels. After the blood preparation was flowed through and the channel was cleaned with PBS, the channel was examined under an LED fluorescent microscope (Axio Lab.A1: Carl Zeiss AG, Oberkochen, Germany) to image the channel and count the fluorescent particles that remained adhered to the walls. Particles were imaged under a 10x magnification lens using a florescent filter (excitation band pass 450-490 nm, emission low pass 515 nm).

The observations were made 0.5 mm from the inlet to avoid any effects due to the specificity of the flow at the entrance. Two images were taken at the same location in each channel, using two different focal points within the channel to ensure that all adhered particles were represented and in focus between the two images (Figure 3 (a) and (b)). The two images were overlaid to produce a combined image (Figure 3(c)). This was then converted to an 8-bit black and white image, sharpened, and converted into a binary image using a threshold that was manually set so that only the particles were visible. Finally, the black and white values were inverted (Figure 3 (d)). A particle counting algorithm in ImageJ was used to extract the size and number of the bright spots in the image. Several sets of images were counted manually to verify the accuracy of the ImageJ particle counting macro, and in all cases, the results differed by less than 10%, and the result from ImageJ was used.

The experiment was performed for four different target mean flow velocities: v = 0, 1.0, 2.0, 3.0, and 6.0 mm/s. The flow rates used to program the syringe pump were calculated for each channel to achieve the desired mean velocity as $Q = \pi v D^2/4$, where D is the measured diameter of the channel in use.

Each blood sample was flowed through a channel for one minute at the flow rate calculated for that channel to achieve the desired velocity. All combinations of flow velocity and dextran concentration were each repeated five to eight times. Each test was performed in a new, clean channel that was fabricated no more than 48 hours beforehand.

As measures of particle margination, we examined the absolute particle counts for each condition, normalized by the averaged counts obtained from the baseline 0% dextran samples. We additionally defined a non-dimensional adhesion coefficient C_a, normalized by the particle flux through the channel as:

$C_a = \frac{c_w}{\mathrm{J_p}}$, where c_w is rate of particle capture at the wall per unit surface area in particles/(s.m^2), $\mathrm{J_p} = \frac{\emptyset\, Q}{\vartheta_\mathrm{p}} \frac{1}{\pi \mathrm{R}^2}$ is the flux of particles through the capillary cross section, also in particles/(s.m^2), $\emptyset$ is the volume faction of particles, Q the flow rate, ϑ_p the volume of a single particle, and R the capillary radius. Assuming a steady condition, C_a was estimated after flowing the solution during T=1 min as:

$C_a = \frac{\int_0^T c_w\, dt}{\int_0^T J_p\, dt}$, where $\int_0^T c_w dt$ is the total count of particles per unit of surface at t=T and $\int_0^T J_p dt$ is the total count of particles that cross the capillary section during t=T. For each trial, a shear rate metric γ (s^{-1}) was calculated from the channel diameter D and average flow velocity v as $\gamma = 4v/D$.

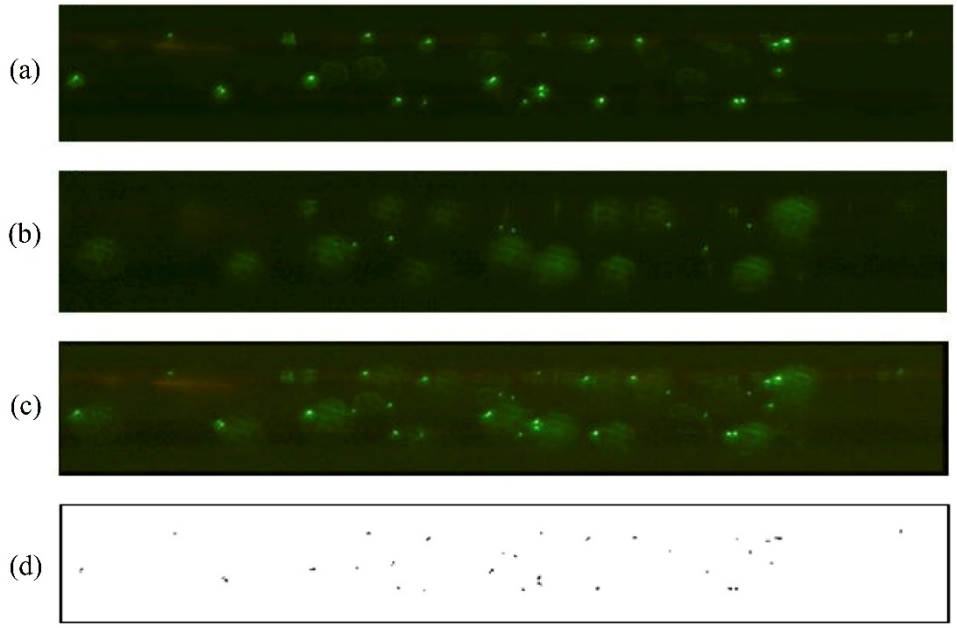

Figure 3. Image processing method used to count particle adhering to channel walls: (a) and (b) original two images taken at different focal distances within the channel; (c) the combined image; (d) the post-processed image used for particle counting.

2 RESULTS AND DISCUSSION

2.1 Effect of dextran on RBC Aggregation

The effect of dextran 500 on the RBC aggregation levels was found to be similar to that previously reported [19]: aggregation was found to increase with increasing dextran concentration up to the 1.5% samples, beyond which it decreased. Fitting a third order polynomial to the measurements (Figure 4), the peak aggregation was more precisely estimated to correspond with concentrations of 1.76% dextran, which is within the range of values previously reported [13,19,20]. The averaged aggregation indices of the different dextran concentrations are reported in Table 1, with the physiological value reported by Baskurt *et al.* listed for reference [19].

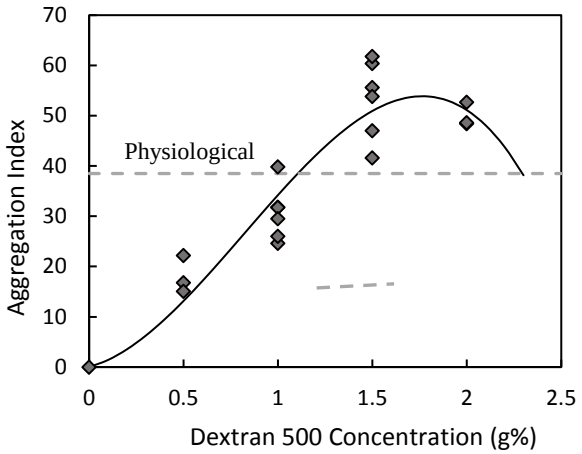

225

226 Figure 4. Aggregation index vs. concentration of dextran 500. A third order polynomial is fitted to the data (continue line).

227 Table 1. Average aggregation indices for increasing dextran concentration. *Physiological value from [19] for the same type of
228 aggregometer..

Dextran Concentrations	Aggregation Index
0.0%	0*
0.5%	18.0 ± 3.7
1.0%	30.6 ± 5.4
1.5%	53.4 ± 7.8
2.0%	49.9 ± 2.4
Physiological*	38.5 ±2.2

229 *2.2 Particle Adherence*

230 The average particle counts, normalized by the averaged results for the 0% dextran concentrations, are
231 presented in Figure 5 for all dextran concentrations and flow velocities tested. The results averaged across
232 the different flow velocities for each dextran concentration are also shown here as hatched bars. Following
233 the same trend of aggregation index *vs.* dextran concentration (Figure 4), with the exception of the 1%

dextran concentration, average particle adherence increases up to 1.5% dextran, and decreases for the 2% dextran samples. Comparing these averaged results using two-tailed t-tests, particles in the preparations that had levels of aggregation below physiological levels (0%, 0.5% and 1.0% dextran) were on average significantly less likely to marginate compared to those in the samples having aggregation levels higher than physiological (1.5% and 2.0% dextran).

This relation between aggregation and particle adherence is further illustrated by Figure 6, in which the normalized adhesion coefficients C_a are plotted against the aggregation indices for the corresponding samples. These results are presented for the lowest flow velocity v=1.0 mm/s, as well as the averaged C_a values for velocities 1, 2, and 3 mm/s. The adhesion coefficient is positively correlated with aggregation index, illustrated by lines of best fit. The slope of the fitted line is higher for the results of the lowest velocity than for those of the averaged velocities, indicating that margination is more sensitive to the aggregation level at lower velocities, and the corresponding lower levels of shear. This result is not surprising, given that RBC aggregation decreases and is eventually inhibited as shear rate increases, so its influence on margination would also be expected to dissipate with increasing velocities and shear.

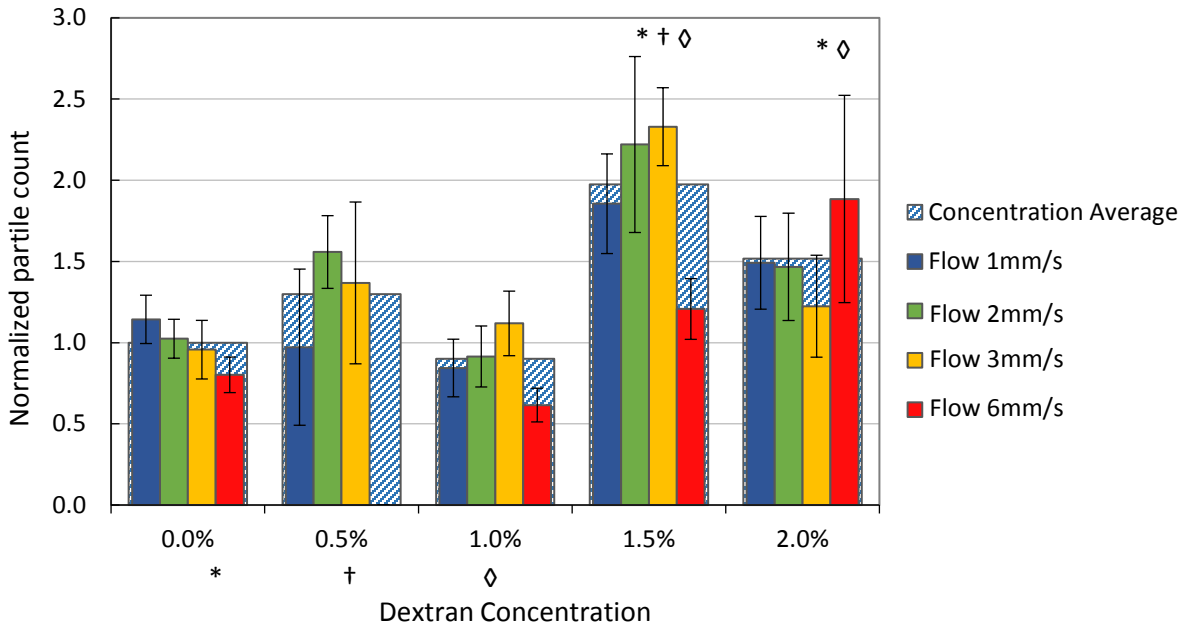

249

250 Figure 5. Averaged normalized counts of binding microparticles for each concentration of dextran 500 and each flow velocity.
251 Particle counts were normalized by the averaged result for the 0% dextran solution (all velocities). Hatched bars present particle
252 counts averaged across all velocities for each dextran concentration. *†◊ above a bar signifies statistically significant difference
253 with the averaged result for the respective dextran concentration ($p < 0.05$).

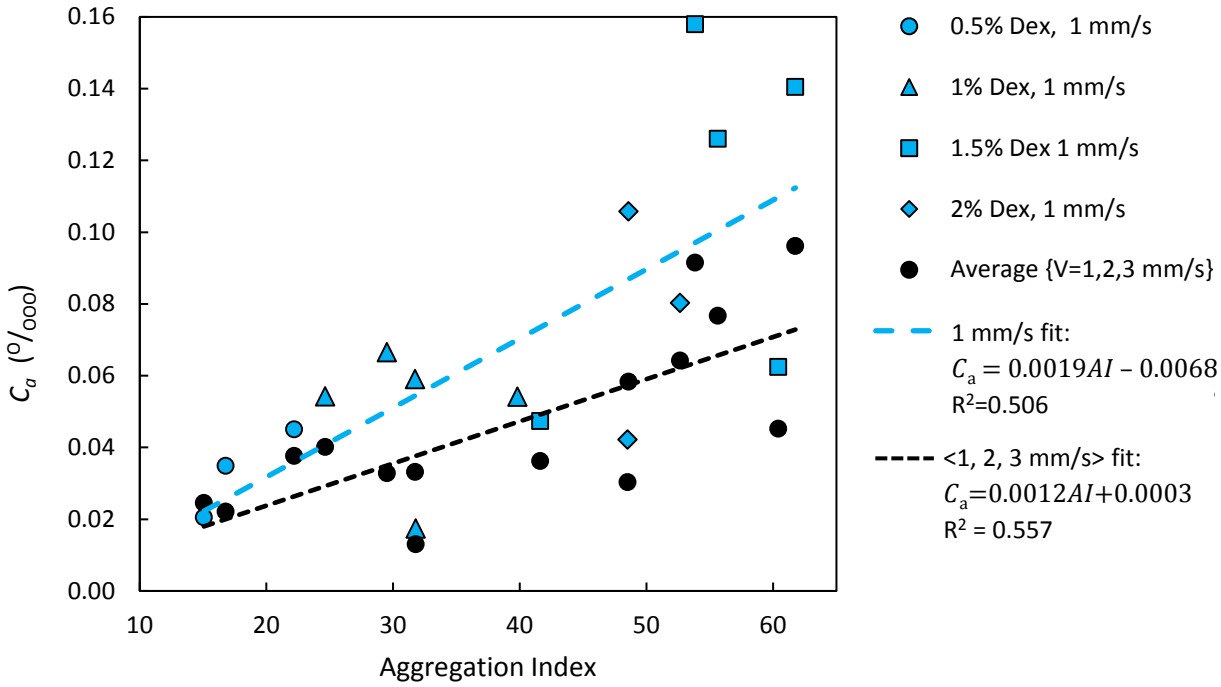

Figure 6. Adhesion coefficient C_a *vs.* corresponding aggregation index for lowest flow v=1 mm/s along with averaged results for v=1, 2, and 3 mm/s. Lines of best fit are presented by dashed lines. °/ooo signifies "per ten thousand", i.e. reflects the number of particles attached per 10,000 particles injected.

From the results of all particle counts shown in Figure 5, we see that the effects of flow velocity on particle adherence vary depending on the dextran concentration. Figure 7 compares the effect of flow velocity on particle adherence in blood samples with no aggregation (0% dextran), maximum aggregation (1.5% dextran) along with the average for all of the aggregating samples (0.5-2.0% dextran). For the non-aggregating samples, there is a moderate negative trend, with particle adherence decreasing monotonically by 30% from velocities 1 mm/s to 6 mm/s. This trend corresponds with other findings that show a negative correlation between shear rate and margination [15] and may be explained by higher by shear forces at the wall that "wash away" some particles and the increase of shear-induced diffusion, which displaces the particles toward the center. According to Taisuke Ota, a single biotin molecule (ligand) forms a bond with

a streptavidin molecule (receptor) with the rupture force between 3.6 and 5.4 pN [REF]. For the presented experiments, the drag force applied by the flow on the spherical particles touching the wall was estimated to fall between 0.7 and 4.4 pN (Stokes flow, viscosity 3.5mPa.s). According to this analysis, the shear is likely responsible for a significate amount of particle detachment.

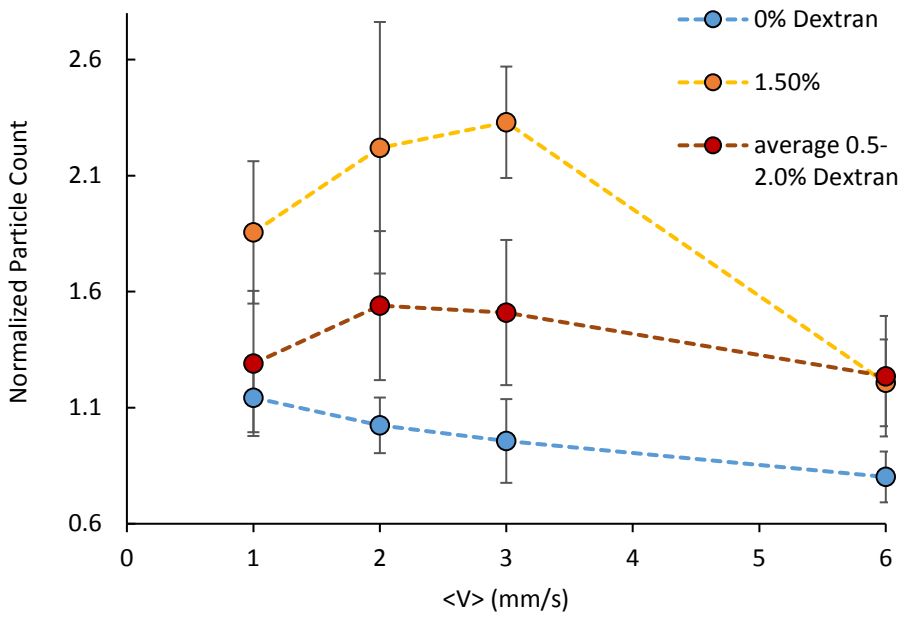

Figure 7. Particle Margination vs. flow velocity. Normalized averaged particle counts vs. average flow velocity for: zero aggregation (0% dextran), maximum aggregation (1.5% dextran) and average for all aggregating samples (0.5-2% dextran).

With the presence of RBC aggregation, the effect of flow velocity on the number of captured particles was significantly altered: in addition to having higher levels of particle adherence overall, unlike for the non-aggregating samples, the relationship for the aggregating samples (1.5% and average concentration) is non-monotonic. Particle adherence increases up to some optimal velocity, beyond which it decreases. For the maximum aggregation level (1.5% dextran), margination was greatest at v=3 mm/s. For the averaged dextran concentrations it was greatest at v=2 mm/s.

When plotting the adhesion coefficient that has been normalized by the particle flux, however (Figure 8), we see that this indicator of margination decreases monotonically with increasing shear rate. This reveals that the maxima observed for aggregating samples in Figure 7 was indeed, consequence of the increased

particle flux associated with the increased flow rates. For aggregating samples, the effects of aggregation, coupled with the increased particle flux, resulted in a net increase in captured particles up to some critical velocity (Figure 7). Above this velocity, the elevated shear forces that inhibit margination also broke up aggregates, eliminating their pro-margination influence, and the number of captured particles decreased. It is reasonable that the critical velocity for maximum particle count was highest for the highest aggregation level, because for theses samples, aggregates would have been larger, on average, and more resistant against shear to break apart, thus prolonging the aggregates influence on margination up to higher flow velocities.

The averaged values of C_a plotted in Figure 8 (c) further show that at low shear rates (<150 s^{-1}) higher levels of aggregation are associated with significant increases in margination. This effect diminishes as the shear rate increases. Again, this result was expected, as at shear rates above 100-120 s^{-1}, RBC aggregation is inhibited and disaggregation occurs [19]. For each concentration of dextran, the dimensionless adhesion coefficients were plotted against the inverse shear rate and fitted with linear regression as $C_a=\alpha/\gamma$, where α is the experimental fit coefficient (Graphs not shown here). The fit coefficients and R^2 values for the five different aggregation levels are listed in Table 2, and the fitted trends for the 0% and 1.5% dextran concentrations are plotted as dashed lines, along with the averaged results in Figure 8 (c). The fit coefficient α represents the sensitivity of the marginating behaviour to the aggregation level. It is relatively constant for the lower aggregation levels (0-1% dextran) but increases significantly in the higher dextran concentrations (>1%) as the mean aggregation index increases (Figure 9). In other words, as aggregation levels increase to near the range of physiological levels, its influence on margination is heightened, particularly at low levels of shear rate. This is presumably due to the larger aggregate sizes associated with the higher aggregation indices and enabled by the lower levels of shear.

For both the red blood cells and particles, the Péclet numbers are high (~1000), and the particle Reynolds numbers are low (~0.0001). This suggests that shear-induced migration dominates Brownian diffusion and inertial lift for these conditions [21]. For monodisperse particles, the shear-induced diffusion is proportional to the product $\gamma D_{P,}^2$ where D_p is the particle diameter [22]. As the RBCs and RBC aggregates

have effective diameters considerably larger than the 1µm particles, their migration toward the center is greater. Therefore, with the core of the vessel predominantly occupied by the RBCs, the particles are left close to the wall. The net effect of shear can be interpreted as a combination of the increase of shear force at the wall that “washes away” some particles and the increase of shear-induced diffusion, which displaces the particles toward the center.

While the behaviour of polydisperse solutions is not yet fully understood, it has been shown that shear-induced migration enables separation of the feed flow [23]. This suggests that RBC aggregation - which increases the effective size of the “blood particles”- enhances segregation of the micro-particles, promoting their attachment to the wall.

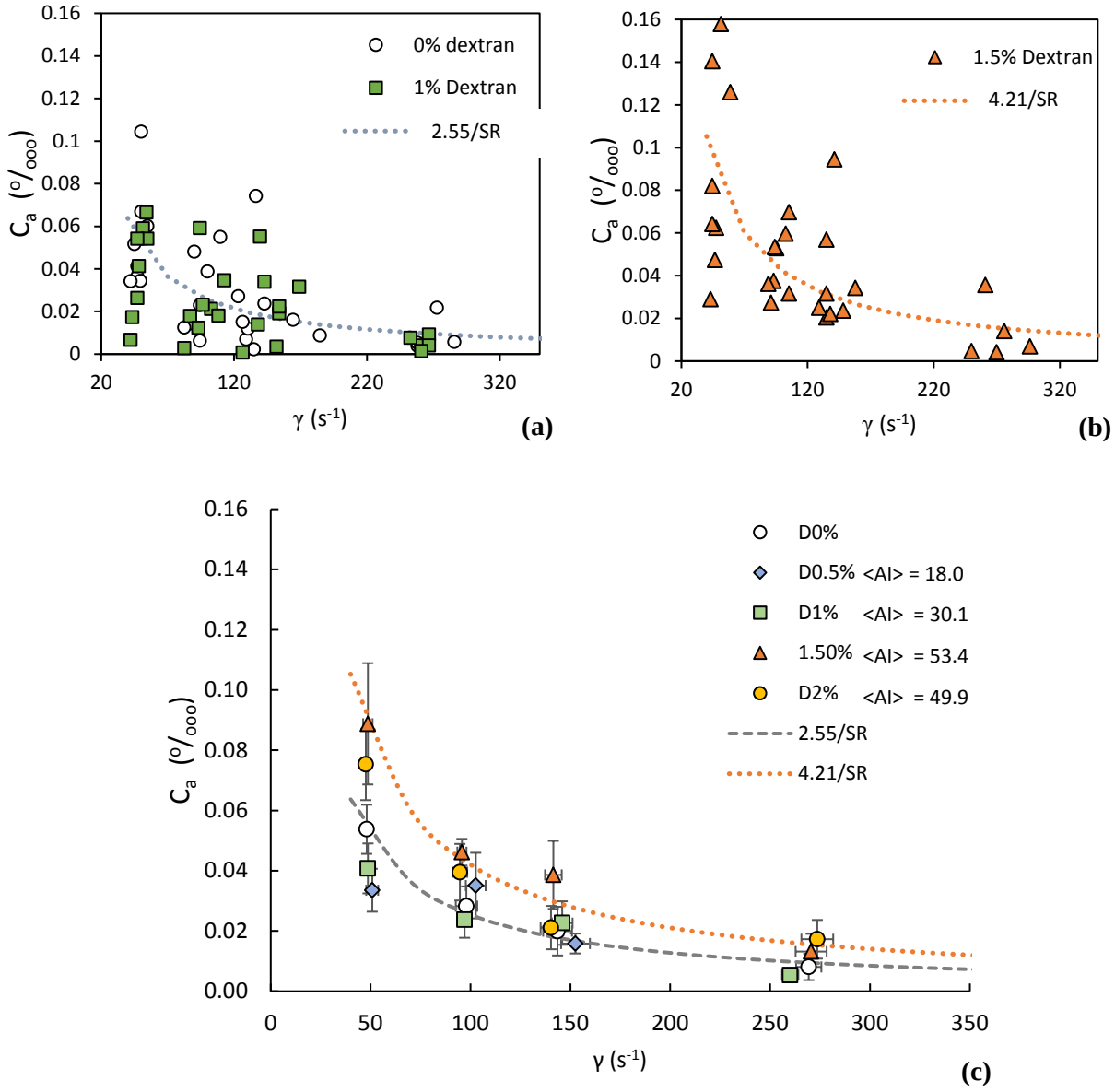

Figure 8. Normalized adhesion coefficient C_a vs. shear rate: (a) for 0% and 1% dextran concentrations; (b) for 1.5% dextran concentration; (c) averaged results for all dextran concentrations. °. °/ooo signifies "per ten thousand", i.e. reflects the number of particles attached per 10,000 particles injected.

330

Table 2: adhesion fit coefficient (α) versus *mean* aggregation indices. * Aggregation index of the 0% dextran samples were set to zero

dextran (w/v)	Mean Aggregation Index	α	R^2	Two-tailed Probability
0%	0*	2.55	0.43	p=0.00004 (N=32)
0.5%	18.0	2.07	0.69	(N=9)
1%	30.6	2.03	0.33	p=0.00125 (N=29)
1.5%	53.4	4.21	0.50	p=0.00002 (N=29)
2%	49.9	3.47	0.71	p=0.0000 03 (N=20)

.

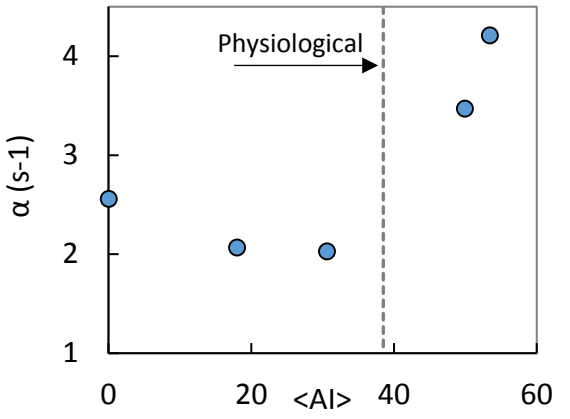

Figure 9. Alpha factor vs. mean aggregation index corresponding to Dextran concentration 0 to 2%.

In this study, we have used particle adhesion as an indicator of particle margination. We note that while closely related to margination, particle adhesion is an imperfect measure of it, as it does not account for particles that may become detached from the wall due to increasing fluid drag or collisions with RBC aggregates [24], or the characteristics of the molecular bonds with receptors in the endothelium [1]. In future studies, investigators may measure the particle distribution in the tube as a more direct measure of margination. We also note that this study of rigid spheres does not account for cell flexibility or the shape of irregular particles such as platelets, and that these variables could account for the contradicting results regarding margination of platelets and similar sized spheres reported in literature. Here, we established the effect of RBC aggregation on the margination of 1 μm rigid spheres within round channels under varying shear rate in the range of physiological conditions. These results may help to delineate the effects of specific platelet characteristics, which may be investigated in future studies. In addition, according to Muller et al. [Muller] particle margination strongly depends on how well particles fit within a cell free layer. Considering

this and that RBC aggregation is known to increase the cell free layer thickness [5], further optimization of particle size should take into account the aggregability of the blood.

3 CONCLUSIONS

The effects of RBC aggregation level on the margination of 1 μm spheres has been quantified within round microchannels (85 μm) under varying physiological levels of shear rate. For the non-aggregating samples (0% dextran) the absolute numbers of captured particles decreased with increasing flow velocity, but for the aggregating samples, particle capture was significantly higher and exhibited a local maximum for a critical velocity. A non-dimensional adhesion coefficient was defined to account for the increased particle flux associated with higher flow rates, and exhibited a monotonic decrease with shear rate for all aggregation levels. Increase in aggregation level resulted in a significant increase in margination for both absolute and dimensionless indicators, particularly at low levels of shear rate ($<150\ s^{-1}$) under which aggregation was strongest. This finding agrees with those of other studies that examined the effect of aggregation on margination within different channel geometries (e.g. a Couette cylinder [25] or parallel plate flow chamber [26]). Margination was found to be especially sensitive to aggregation level in the range of physiological aggregation levels of whole blood (most notably for the 1.5% dextran concentration). This indicates that aggregation plays an important role in physiological margination. It has already been shown that aggregation plays an important role in the human body's immune system [27], and the presented results indicate that one mechanism by which it does this is by increasing margination, which can help platelets and immune cells travel to the site of inflammation to support the healing and immune defense process. This potentially explains why an increase in aggregation is so often observed in different pathological conditions. These findings could be used better understand the roles of aggregation and margination in the body and their importance toward inflammation and immune response.

Conflict of interest

The authors have no conflicts of interest.

Ethical approval

The study was conducted with the with the approval of the University of Ottawa ethics committee (H11-13-06)

Acknowledgment This work was funded by the National Science and Engineering Research Council of Canada (#RGPIN-2015-06188). This work was also supported by the Canada Foundation for Innovation (#31112).

References

[1] Carboni E, Tschudi K, Nam J, Lu X, Ma AWK. Particle Margination and Its Implications on Intravenous Anticancer Drug Delivery. AAPS PharmSciTech 2014;15:762–71. doi:10.1208/s12249-014-0099-6.

[2] Kumar A, Graham MD. Margination and segregation in confined flows of blood and other multicomponent suspensions. Soft Matter 2012;8:10536–48. doi:10.1039/c2sm25943e.

[3] Hou HW, Bhagat AAS, Han J, Lim CT. Deformability based cell margination - A simple microfluidic design for malarial infected red blood cell filtration. IFMBE Proceedings, vol. 31 IFMBE, 2010, p. 1671–4. doi:10.1007/978-3-642-14515-5_424.

[4] Hur SC, Henderson-Maclennan NK, McCabe ERB, Di Carlo D. Deformability-based cell classification and enrichment using inertial microfluidics. Lab on a Chip 2011;11:912–20. doi:10.1039/c0lc00595a.

[5] Charoenphol P, Onyskiw PJ, Carrasco-Teja M, Eniola-Adefeso O. Particle-cell dynamics in human blood flow: Implications for vascular-targeted drug delivery. Journal of Biomechanics 2012;45:2822–8. doi:10.1016/j.jbiomech.2012.08.035.

[6] Nobis U, Pries AR, Cokelet GR, Gaehtgens P. Radial distribution of white cells during blood flow in small tubes. Microvascular Research 1985;29:295–304. doi:10.1016/0026-2862(85)90020-2.

[7] Tilles AW, Eckstein EC. The near-wall excess of platelet-sized particles in blood flow: Its dependence on hematocrit and wall shear rate. Microvascular Research 1987;33:211–23. doi:10.1016/0026-2862(87)90018-5.

[8] Aarts PA, van den Broek SA, Prins GW, Kuiken GD, Sixma JJ, Heethaar RM. Blood platelets are concentrated near the wall and red blood cells, in the center in flowing blood. Arteriosclerosis, Thrombosis, and Vascular Biology 1988;8:819–24. doi:10.1161/01.ATV.8.6.819.

[9] Yeh C, Eckstein EC. Transient lateral transport of platelet-sized particles in flowing blood suspensions. Biophysical Journal 1994;66:1706–16. doi:10.1016/S0006-3495(94)80962-2.

[10] Vejlens G. The distribution of leukocytes in the vascular system. Acta Pathol Microbial Scand 1938;33:159–90.

[11] Fedosov DA, Fornleitner J, Gompper G. Margination of White blood cells in microcapillary flow. Physical Review Letters 2012;108:1–5. doi:10.1103/PhysRevLett.108.028104.

[12] Freund JB. Leukocyte margination in a model microvessel. Physics of Fluids 2007;19. doi:10.1063/1.2472479.

[13] Pearson MJ, Lipowsky HH. Influence of erythrocyte aggregation on leukocyte margination in postcapillary venules of rat mesentery. Am J Physiol Heart Circ Physiol 2000:1460–71. doi:10.1152/ajpheart.2000.279.4.H1460.

[14] Woldhuis B, Tangelder GJ, Slaaf DW, Reneman RS. Influence of dextrans on platelet distribution in arterioles and venules. Pflügers Archiv European Journal of Physiology 1993;425:191–8. doi:10.1007/BF00374166.

[15] Guilbert C, Chayer B, Allard L, Yu FTH, Cloutier G. Influence of erythrocyte aggregation on radial migration of platelet-sized spherical particles in shear flow. Journal of Biomechanics 2017;61:26–33. doi:10.1016/j.jbiomech.2017.06.044.

[16] Jain A, Munn LL. Determinants of leukocyte margination in rectangular microchannels. PLoS ONE 2009;4:1–8. doi:10.1371/journal.pone.0007104.

[17] Goldsmith HL, Spain S. Margination of Leukocytes in Blood-Flow through Small Tubes. Microvasc

Res 1984;27:204–22. doi:Doi 10.1016/0026-2862(84)90054-2.

[18] Yang X, Forouzan O, Burns JM, Shevkoplyas SS. Traffic of leukocytes in microfluidic channels with rectangular and rounded cross-sections. Lab on a Chip 2011;11:3231–40. doi:10.1039/c1lc20293f.

[19] Baskurt OK, Neu B, Meiselman HJ. Red Blood Cell Aggregation. CRC Press; 2012.

[20] Neu B, Wenby R, Meiselman HJ. Effects of Dextran Molecular Weight on Red Blood Cell Aggregation. Biophysical Journal 2008;95:3059–65. doi:10.1529/biophysj.108.130328.

[21] Schroën K, van Dinther A, Stockmann R. Particle migration in laminar shear fields: A new basis for large scale separation technology? Separation and Purification Technology 2017;174:372–88. doi:10.1016/j.seppur.2016.10.057.

[22] Eckstein EC, Bailey DG, Shapiro AH. Self-diffusion of particles in shear flow of a suspension. Journal of Fluid Mechanics 1977;79:191–208. doi:10.1017/S0022112077000111.

[23] Shauly A, Wachs A, Nir A. Shear-induced particle resuspension in settling polydisperse concentrated suspension. International Journal of Multiphase Flow 2000;26:1–15. doi:10.1016/S0301-9322(98)00086-X.

[24] Nash GB, Watts T, Thornton C, Barigou M. Red cell aggregation as a factor influencing margination and adhesion of leukocytes and platelets. Clinical Hemorheology and Microcirculation 2008;39:303–10. doi:10.3233/CH-2008-1109.

[25] Guilbert C. Influence de l'agrégation érythrocytaire sur la migration axiale de microparticules simulant des plaquettes sanguines. 2009. doi:10.1007/s13398-014-0173-7.2.

[26] Namdee K, Thompson AJ, Charoenphol P, Eniola-Adefeso O. Margination propensity of vascular-targeted spheres from blood flow in a microfluidic model of human microvessels. Langmuir 2013;29:2530–5. doi:10.1021/la304746p.

[27] Baskurt OK, Boynard M, Cokelet GC, Connes P, Cooke BM, Forconi S, et al. New guidelines for hemorheological laboratory techniques. Clinical Hemorheology and Microcirculation 2009. doi:10.3233/CH-2009-1202.